Electrical Power and Energy Systems 42 (2012) 644–652

Contents lists available at SciVerse ScienceDirect

Electrical Power and Energy Systems

journal homepage: www.elsevier.com/locate/ijepes

Differential evolution applied for anticipatory load shedding with voltage stability considerations

L.D. Arya [a], Pushpendra Singh [b], L.S. Titare [c,*]

[a] Department of Electrical Engg., SGSITS, 23-Park Road, Indore, MP 452 003, India
[b] Department of Electrical Engg., VITS, Satna, MP 485 001, India
[c] Department of Electrical Engg., Govt. Engineering College, Jabalpur, MP 482 010, India

ARTICLE INFO

Article history:
Received 12 July 2011
Received in revised form 17 January 2012
Accepted 9 April 2012
Available online 15 June 2012

Keywords:
Proximity indicator
Sensitivity
Load shedding
Voltage stability
Minimum eigenvalue
Differential evolution

ABSTRACT

This paper presents an anticipatory load shedding methodology which determines optimum load shedding at selected buses under emergency based on voltage stability. Accurate load shedding saves loss of revenue to power utility in addition to avoiding voltage instability problem. The buses for load shedding have been selected based on the sensitivity of minimum eigenvalue of load flow Jacobian with respect to load shed. A computational algorithm for minimum load shedding has been developed using DE. The algorithm accounts inequality constraints not only in present operating condition but also for predicted next interval load. Developed algorithm has been implemented on IEEE 6-bus and 14-bus test systems. Results have been compared with those obtained using particle swarm optimization (PSO) and its variant based on statistical inference.

1. Introduction

Fault, sudden dramatic load change, and insufficient generation can create power mismatch between generation and loads. If generation in power systems is insufficient to power all loads, efficient load shedding operations may need to be deployed to maintain the supply–demand balance. Load shedding is the process of tripping certain amount of load with lower priority to maintain the stability of the remaining portion of the system [1]. In many practical situations load shedding is initialized by the under voltage relays [2]. It has been established that under voltage criterion has poor discriminative ability and in fact proper discrimination for load-shed may be obtained from voltage stability margin view point [3]. Load-shed criterion may be based on some proximity indicator whose magnitude indirectly reflects the stability margin and provides information for initialization of load shedding. Under such situation the magnitude of the indicator may be monitored during normal operating condition and when it falls below a threshold value, alarm should be actuated. If the indicator continues to decline and reaches to another lower value of load shedding is to be initiated. Such situation may arise due to (i) sudden loss of generation/increase in load which may result in decrease in frequency; (ii) outage of one or more transmission line thus reducing network loadability and may cause load bus limit violations; and (iii) Overloading of transmission line. Network loadability is used here as the loadability from voltage stability viewpoint and transmission line overloading is the overloading when transmission line flow violates the specified thermal limit of the line. In view of this load shedding may be adopted based on (i) under frequency consideration [4], (ii) Overload alleviation of transmission lines [5], and (iii) voltage limit violation/voltage stability consideration [6]. Limited research work has been done on load shedding to avoid risk of voltage collapse. A load shedding strategy that maximizes the system reactive security margin has been developed by Berg and Sharaf [6]. The methodology is based on nonlinear optimization formulation. Tuan et al. [7] presented a viable load shedding algorithm which determines the load to be shed based on sensitivity of indicator with respect to load. El-Sadek et al. [8] developed a methodology for optimum load shedding using L-indicator under emergency to avoid voltage instability problem. Successive load flow runs are required to accomplish proposed technique. Bijwe et al. [9] developed an anticipatory load shedding technique using LP formulation for loadability enhancement. Luan et al. [10] developed optimal load shedding algorithm using genetic algorithm for distribution network. Jung et al. [11] described an application of multi-agent system for development of a new defense system for assessment of power system vulnerability and perform self healing corrective and preventive control action. Conventionally

* Corresponding author.
E-mail addresses: ldarya@rediffmail.com (L.D. Arya), erpsingh@rediffmail.com (P. Singh), lstitare@yahoo.co.in (L.S. Titare).

0142-0615/$ - see front matter © 2012 Elsevier Ltd. All rights reserved.
http://dx.doi.org/10.1016/j.ijepes.2012.04.006

Nomenclature

J	objective function
ls_i	total load shed at ith load bus
NLS	set of load buses selected for load shedding
P,Q	real and reactive power flow
$\lambda_{\min}$	minimum eigenvalue of load flow Jacobian
$\lambda_{\min}^{th}$	threshold value of minimum eigenvalue of load flow Jacobian
$\lambda_{\min}^{o}$	minimum eigenvalue of load flow Jacobian under current operating condition accounting load shed
$\lambda_{\min}^{p}$	minimum eigenvalue of load flow Jacobian under predicted load condition accounting load shed
$\underline{P}_{gk}, \underline{Q}_{gk}$	lower bound on active and reactive power generation at kth bus
$\overline{P}_{gk}, \overline{Q}_{gk}$	upper bound on active and reactive power generation at kth bus
P_{gk}^{o}, Q_{gk}^{o}	active and reactive power generation at kth bus under current operating condition accounting load shed
P_{gk}^{p}, Q_{gk}^{p}	active and reactive power generation at kth bus under predicted load condition accounting load shed
NG	total number of generator buses
V_i^{o}	load bus voltage at ith load bus under current operating condition accounting load shed
V_i^{p}	load bus voltage at ith load bus under predicted load condition accounting load shed
$\underline{V}_i, \overline{V}_i$	lower and upper bound on ith load bus voltage

two approaches are adopted for load shedding namely, (i) shed a predetermined amount of load if the observed voltage/frequency falls below a threshold value and (ii) load shedding is based on the rate of voltage/frequency decline. But a convergence criteria of the reinforcement-learning technique (combines the above mentioned two conventional load shedding methods) is applied to implement constrained load shedding agent for determining optimal load shedding. Change in the load shedding agent based on the voltage/frequency decline. However, the load shedding agent examines the rate of voltage/frequency decline to determine the amount of the load to be shed under current operating condition. Echavarren et al. [12] presented a LP based optimization algorithm for load shedding to improve load margin considering first order margin sensitivities. Chattopadhyay and Chakraborti [13] presented a preventive control model to prevent voltage instability accounting dynamics of load shedding. Amraee et al. [14] developed an optimal load shedding algorithm which is based on the concept of the static voltage stability margin and its sensitivity at the maximum loading point. Girgis and Mathure [15] presented a methodology that shows the rate of change of frequency can be utilized to determine the magnitude of generation–load imbalance, while the rate of change of voltage with respect to active power can be utilized to identify the sensitive bus for load shedding. Fu and Wang [16] presented an algorithm for studying the load shedding problem in emergencies where an ac power flow solution cannot be found for the stressed system. Amraee et al. [17] proposed an adaptive under voltage load shedding scheme using model predictive control to protect power system against voltage instability. In this paper a new anticipatory load shedding algorithm based on voltage stability considerations using differential evolution has been proposed. Minimum eigenvalue is used as an indicator. A threshold value of this indicator can be assumed for a specific system based on operating experience. Emergency load shedding is required if this value falls below the threshold value. Optimal load shedding algorithm which consists of two parts one of it identifies load buses for load to be shed and the other determines the optimum load to be shed at selected buses using differential evolution. Load buses having large sensitivities are selected for load shedding. Operating constraints on the load to be shed are accounted under current operating condition and for predicted next interval load. Due to operating constraints there is a maximum limit to the load that can be shed at the selected buses to ensure a minimum service. Section 2 presents problem formulation. Section 3 gives an overview of DE technique, bounce back technique and handling of inequality constraints. Section 4 presents implementation of the developed algorithm for optimizing objective function. Section 5 presents results and discussions. Section 6 gives conclusions and highlights of the paper.

2. Problem formulation

The objective function is to minimize total load shed at current operating condition.

$$J = \sum_{i=NLS} ls_i \tag{1}$$

Above objective function is optimized subject to following constraints:

(i) Power flow constraints under current operating condition as well as next predicted loading condition accounting load shed:

$$\begin{aligned} \underline{P} &= \underline{f}(\underline{V}, \delta) \\ \underline{Q} &= \underline{g}(\underline{V}, \delta) \end{aligned} \tag{2}$$

It is stressed that power flow is performed under current operating condition as well as at next predicted loading condition after the load shed.

(ii) Inequality constraint on minimum eigenvalue of load flow Jacobian at current operating point as well as next predicted load condition accounting load shed:

$$\begin{aligned} \lambda_{\min}^{o} &\geqslant \lambda_{\min}^{th} \\ \lambda_{\min}^{p} &\geqslant \lambda_{\min}^{th} \end{aligned} \tag{3}$$

(iii) Active power generation constraint under base case condition as well as at next predicted loading condition accounting load shed:

$$\begin{aligned} &\underline{P}_{gk} \leqslant P_{gk}^{o} \leqslant \overline{P}_{gk} \\ &\underline{P}_{gk} \leqslant P_{gk}^{p} \leqslant \overline{P}_{gk} \\ &\quad k = 1, 2, \ldots, NG \end{aligned} \tag{4}$$

(iv) Reactive power generation constraint under base case condition as well as at next predicted loading condition accounting load shed:

$$\begin{aligned} &\underline{Q}_{gk} \leqslant Q_{gk}^{o} \leqslant \overline{Q}_{gk} \\ &\underline{Q}_{gk} \leqslant Q_{gk}^{p} \leqslant \overline{Q}_{gk} \\ &\quad k = 1, 2, \ldots, NG \end{aligned} \tag{5}$$

(v) Inequality constraint on load bus voltages in present as well as for next predicted interval load that is load bus voltage with in limit accounting load shed:

$$\underline{V}_i \leqslant V_i^o \leqslant \overline{V}_i$$
$$\underline{V}_i \leqslant V_i^p \leqslant \overline{V}_i \quad (6)$$
$$i = NG+1, \ldots, NB$$

(vi)

$$\underline{ls}_i \leqslant ls_i \leqslant \overline{ls}_i \quad i \in NLS \quad (7)$$

ls_i is the amount of total load shed and $\overline{ls}_i$ denotes maximum permissible load shed at ith bus. In fact permissible load shedding is a fraction of total load at selected bus. It may be, say 80% of the total load and rest 20% may be a load which is required in emergency condition. This depends on utility policy.

It is stressed that load shedding is performed at current loading condition. Further, constraints as in Eqs. (3)–(6) are ascertained by performing load flow solution at current operating condition (after load shedding) and predicted load condition (accounting load shed).

3. Differential evolution: an overview

Differential evolution (DE) is a very simple population based, stochastic function minimizer and has been found very powerful to solve various nature of engineering problems [18–20]. DE optimizes the problem by sampling the objective function at multiple randomly chosen initial points. Preset parameter bounds define the region from which 'M' vectors in this initial population are chosen. DE generates new solution points in 'D' dimensional space that are perturbations of existing points. It perturbs vectors with the scaled difference of two randomly selected population vectors. To produce a mutated vector, DE adds the scaled, random vector difference to a third selected population vector (called as base vector). Further DE also employs a uniform crossover to produce trial vector from target vector and mutated vector. The three fundamental steps are explained below:

Step-(a) Initialization: Initial population of size 'M' is generated as follows:

$$ls^0 = \left[x_1^0, x_2^0, x_3^0, \ldots, x_M^0\right]$$
$$x_i^0 = \left[ls_{i,1}^0, ls_{i,2}^0, ls_{i,3}^0, \ldots, ls_{i,NLS}^0\right]^T \quad (8)$$

ls_{ij}^0 i.e. jth parameter of x_i vector is obtained from uniform distribution as follows:

$$ls_{i,j}^0 = \underline{ls}_j + (\overline{ls}_j - \underline{ls}_j) rand_j \quad (9)$$

$\underline{ls}_j$ and $\overline{ls}_j$ are lower and upper bounds on variable ls_j.
$rand_j$ is a random digit in the range [0, 1].

Step-(b) Mutation: DE mutates and recombines the population to produce a population of 'M' trial vectors. Differential mutation adds a scaled, randomly sampled, vector difference to a third vector as follows:

$$\underline{\rho}_i^{(k)} = ls_{base}^{(k)} + \alpha\left(ls_p^{(k)} - ls_q^{(k)}\right) \quad (10)$$

α is known as scale factor usually lies in the range [0, 1],
$ls_p^{(k)}$ and $ls_q^{(k)}$ are two randomly selected vectors (p?q).
$ls_{base}^{(k)}$ is known as base vector.
$\underline{\rho}_i^{(k)}$ is a mutant vector.

The base vector index 'b' may be determined in variety of ways. This may be a randomly chosen vector ($base$?p?q).

Step-(c) Crossover: DE employs a uniform crossover strategy. Crossover generates trial vectors $t_i^{(k)}$ as follows:

$$t_{i,j}^{(k)} = \begin{cases} \rho_{i,j}^{(k)}, & \text{if}(rand_j \leqslant C_r or \cdot j = j_{rand}) \\ ls_{i,j}^{(k)}, & \text{Otherwise} \end{cases} \quad (11)$$

C_r is a crossover probability lies in the range [0, 1]. C_r is a user defined value which controls the number of parameter values which are copied from the mutant. If the random number $rand_j$ is less than or equal to C_r, the trial parameter is adopted from the mutant $\rho_i^{(k)}$. Further, the trial parameter with randomly chosen index, j_{rand} is taken from the mutant to ensure that trial vector does not duplicate target vector ls_i^k. Otherwise the parameter is adopted from the target vector ls_i^k.

Step-(d) Selection: Objective function is evaluated for target vector and trial vector, trial vector is selected if it provides better value of the function than target vector as follows:

$$ls_i^{(k+1)} = \begin{cases} t_i^{(k)}, & \text{if}\left[f\left(t_i^{(k)}\right) \leqslant f\left(ls_i^{(k)}\right)\right] \\ ls_i^{(k)}, & \text{Otherwise} \end{cases} \quad (12)$$

The process of mutation, crossover and selection is executed for all target vector index 'i' and a new population is created till the optimal solution is obtained. The procedure is terminated if a maximum number of generations (k) have been executed or no improvement in objective function is noticed in a pre-specified generations. Various benchmark versions of DE that differ in the new generation methods largely are available [19]. In this paper DE/best/1/bin has been selected. The first term after DE i.e. 'best' specifies the way base vector is chosen. In this selected scheme the base vector is the current best so far vector. '1' After best denotes that one vector difference contributes to the differential. Last term 'bin' denotes binomial distribution that result because of uniform crossover. Number of parameters donated by mutant vector closely follows binomial distribution. It is to be noted that best, target and difference vector indices are all different.

3.1. Bounce back technique for handling bounds on decision variables

Some of the variables may cross the lower or upper bounds in a mutant vector $\rho_i^{(k)}$ in executing differential as governed by relation (10). Bounce back mechanism is adopted to bring such decision variables within limit. The bounce-back method replaces element which has violated limits by the new element whose value lies between the base parameter value and the bound being violated. The following relations are used for violated mutant vector elements [19].

$$\rho_{i,j}^{(k)} = \begin{cases} ls_{base,j} + rand \cdot (\underline{ls}_j - ls_{base,j}), & \text{if}\left(\rho_{i,j}^{(k)} \leqslant \underline{ls}_j\right) \\ ls_{base,j} + rand \cdot (\overline{ls}_j - ls_{base,j}), & \text{if}\left(\rho_{i,j}^{(k)} > \overline{ls}_j\right) \end{cases} \quad (13)$$

3.2. Handling of inequality constraints

A direct inequality constraint handling technique devised by Lampinen [21] has been adopted in this paper. In its simple form Lampinen's criterion selects {step (d)} the trial vector $t_i^{(k)}$ under following conditions:

(i) $t_i^{(k)}$ satisfies all constraints and has a lower or equal value of objective function than $ls_i^{(k)}$.
(ii) $t_i^{(k)}$ is feasible and $ls_i^{(k)}$ is not feasible.
(iii) $t_i^{(k)}$ and $ls_i^{(k)}$ are both infeasible, but $t_i^{(k)}$ does not violet any constraint more than $ls_i^{(k)}$. Otherwise $ls_i^{(k)}$ is retained in the new population.

4. Implementation of differential evolutionary algorithm to solve formulated problem

Step-1: Data input; Reactive power control variables and system parameters (resistance, reactance, and susceptance, etc.).
Step-2: Base case load flow solution is obtained using continuation power flow methodology.
Step-3: Next interval load is predicted.
Step-4: Obtain load flow solution for the predicted next interval load.
Step-5: Obtain sensitivities using relation (A.3) in Appendix A, for selection of most critical load buses.
Step-6: Initialization; Generate population of size '*M*' for load shedding. Generated population is uniformly distributed in the range $[0, \overline{ls_i}]$.

$$x_i^{(0)} = \left[ls_{i,1}^{(0)}, ls_{i,2}^{(0)}, \ldots, ls_{i,NLS}^{(0)}\right]^T, \quad i = 1, 2, \ldots, M$$

Step-7: Run continuation power flow program for each vector of the population and monitor all inequality constraints (2)–(6). If a vector satisfies the constraints call it 'F' (feasible). Otherwise call it 'NF' (not- feasible).
Step-8: Calculate objective function for the feasible vectors.
Step-9: Based on the value of objective function, identify the best solution vector ls_{best}. This is selected as base vector.
Step-10: Set generation count $k = 1$.
Step-11: Select target vector $i = 1$.
Step-12: Select two vectors ls_p and ls_q such that $p \neq q \neq i \neq best$.
Step-13: Generate a mutated vector $\rho_i^{(k)}$ using relation (10).
Step-14: If any component of mutated vector i.e. $\rho_i^{(k)}$ violets the bounds on decision variable (ls_j) then apply bounce back technique using relation (13) and bring the violated variables within limit.
Step-15: Apply uniform crossover using relation (11) to get trial vector $t_i^{(k)}$. If the trial vector satisfy load shedding inequality constraint (7) call it 'F' otherwise 'NF'.
Step-16: Apply Lampinen's criteria as explained in Section 3.2 to select $t_i^{(k)}$ in new population or reject it to retain $ls_i^{(k)}$ in new population.
Step-17: Increase target vector $i = i + 1$, if $i \leqslant M$, repeat from step-12. Otherwise increase generation count $k = k + 1$
Step 18: If $k \leqslant k_{\max}$, repeat from step-11. Otherwise stop.

The implementation described above is applied in sequence to solve formulated problem. Solution of the problem gives anticipatory optimum load shedding at critical load buses based on sensitivity.

5. Results and discussions

The developed algorithm has been implemented for generating load shedding strategies for IEEE 6-bus and 14-bus test systems [22]. For this purpose system has been stressed by uniform loading such that proximity indicator has been reduced to very small value and there is severe violation of bus voltages. Under this simulated stressed systems condition, all other control means are exhausted. In our test system, one such constraint is incorporated, that is, maximum 80% of initial load on the bus can be shed (20% is always supplied for emergency services). Other constraints can be easily incorporated in algorithm by limiting load shedding to prescribed condition.

5.1. 6-Bus system

This system consists of two generator buses and four load buses. The desired range of load bus voltage is 0.95 pu–1.05 pu. Table 1 shows system load, PV-bus voltages, load bus voltages, value of proximity indicator under simulated stressed condition, and static voltage stability limit. In this work a piecewise method is adopted to handle this situation. Set value of indicator is increased in small steps till drastic change (switching back to PV bus) in indicator is observed. From operational experience of system threshold value of indicator is selected as $\lambda_{\min}^{th} = 0.6100$. Table 2 shows evaluated sensitivities using Eq. A.3 at all PQ buses (except at no load PQ buses). Load buses which having higher sensitivities are selected for load shedding. Selected buses are shown as star marked in Table 2. Initially, 3000 populations (0–80% of individual load bus capacity) for each selected load bus have been generated randomly using Excel software according probability distribution of disturbance variables. Continuation power flow was carried out and only 29 sets of particles (Total load is to be shed) of all selected load bus were selected which satisfied all inequality constraints {Eqs.

Table 1
Load flow solution for 6-bus test system under stressed condition. Total load (S_{dt}) = 2.2024 pu, proximity indicator ($\lambda_{\min}$) = 0.2827, static voltage stability limit. = 2.3557 pu.

Bus no.	Bus voltage (pu)		Load (pu)	
1	V_1	1.0878	S_{d1}	0.0000
2	V_2	1.0680	S_{d2}	0.0000
3	V_3	0.8120	S_{d3}	0.8972
4	V_4	0.8357	S_{d4}	0.0000
5	V_5	0.8053	S_{d5}	0.5553
6	V_6	0.7995	S_{d6}	0.7938

Table 2
Load bus ranking according sensitivity of minimum eigenvalue of load flow Jacobian with respect to system load for 6-bus system.

Sr. no.	Load bus	Sensitivity
1	5	0.3292[a]
2	3	0.2394[a]
3	6	0.2195
4	4	0.0000

[a] Load buses selected for load shedding.

Table 3
Effect of DE parameters on optimization of objective function and number of iteration required for convergence for 6-bus test system.

Case	C_r	α	J	No. of iterations for convergence
1	0.40	0.80	0.5863	782
2	0.40	0.75	0.5829	564
3	**0.40**	**0.70**	**0.5818**	**649**
4	0.45	0.80	0.5878	763
5	0.45	0.75	0.5889	577
6	0.45	0.70	0.5835	649
7	0.50	0.80	0.5920	721
8	0.50	0.75	0.5866	748
9	0.50	0.70	0.5828	729
10	0.55	0.80	0.6018	521
11	0.55	0.75	0.5899	671
12	0.55	0.70	0.5847	539
13	0.60	0.80	0.5945	571
14	0.60	0.75	0.5962	581
15	0.60	0.70	0.5842	656
16	0.60	0.85	0.5976	683
17	0.65	0.80	0.5823	632
18	0.65	0.75	0.5957	687
19	0.65	0.70	0.5839	786
20	0.65	0.85	0.5826	765

Bold face number indicates minimum value of objective function has been achieved in 649 iterations with C_r = 0.40 and α = 0.70.

Table 4
Bus voltages and load on load bus after load shedding with and without optimization techniques for 6-bus test system.

Bus no.	Without optimization				With optimization load shedding					
	Base case		Best initial solution based load shedding		DE		PSO		CAPSO	
	Load (pu)	Voltage (pu)	Load (pu)	Voltage (pu)	Load (pu)	Voltage (pu)	Load (pu)	Voltage (pu)	Load (pu)	Voltage (pu)
1	0.0000	1.0878	0.0000	1.0878	0.0000	1.0878	0.0000	1.0878	0.0000	1.0878
2	0.0000	1.0680	0.0000	1.0680	0.0000	1.0680	0.0000	1.0680	0.0000	1.0680
3	0.8972	0.8120	0.6909	0.9573	0.7459	0.9505	0.7063	0.9500	0.6950	0.9525
4	0.0000	0.8357	0.0000	0.9726	0.0000	0.9643	0.0000	0.9659	0.0000	0.9676
5	0.5553	0.8053	0.1286	0.9812	0.1705	0.9781	0.1580	0.9726	0.1699	0.9726
6	0.7938	0.7995	0.7938	0.9574	0.7938	0.9500	0.7938	0.9501	0.7938	0.9500

Table 5
Optimum load shedding at selected load buses using DE, CAPSO and PSO techniques for 6-bus system.

Sr. no.	Optimization technique	Amount of load shedding at selected load bus (pu)				Objective function (pu)
		Bus no. 5		Bus no. 3		
		Pd_5 (pu)	Qd_5 (pu)	Pd_3 (pu)	Qd_3(pu)	
1	DE	0.3224	0.2121	0.1290	0.1550	0.5818
2	CAPSO	0.3363	0.1892	0.1813	0.1405	0.6136
3	PSO	0.3531	0.1866	0.1702	0.1370	0.6153

Table 6
Comparison of differential evolution method with CAPSO and PSO techniques based on statistical inference for 6-bus test system.

Optimization techniques	Arithmetic mean value of the objective function ($\bar{J}$)	Standard deviation of objective function (σ)	Best value of objective function (J_{best})	Worst value of objective function (J_{worst})	Frequency of convergence	Confidence level (γ)	Determined value for the engg. application (c)	Standard error of the mean objective function (ε)	Confidence interval of the objective function (μ)	Length of confidence interval of the objective function (L)
DE	0.5882	0.0059	0.5818	0.6018	12	0.95	2.0452	0.0026	$0.5791 \leqslant \mu \leqslant 0.5845$	0.0110
CAPSO	0.6177	0.0060	0.6136	0.6347	10	0.95	2.0452	0.0027	$0.6150 \leqslant \mu \leqslant 0.6204$	0.0112
PSO	0.6209	0.0062	0.6153	0.6394	09	0.95	2.0452	0.0029	$0.6181 \leqslant \mu \leqslant 0.6237$	0.0115

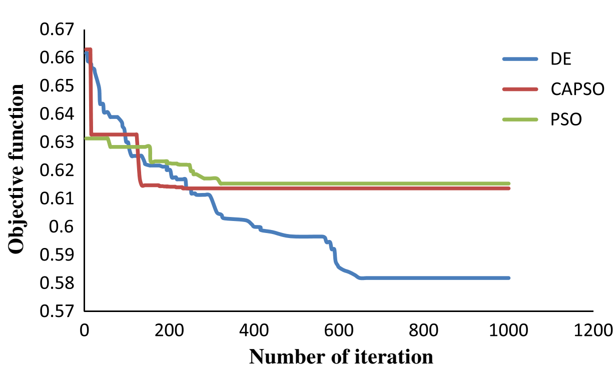

Fig. 1. Plot of convergence of objective function with respect to number of iteration using DE, CAPSO and PSO algorithm for 6-bus system.

Table 7
Load flow solution for 14-bus test system under stressed condition. Total load (S_{dt}) = 5.3015 pu, proximity indicator (λ_{min}) = 0.2705, static voltage stability limit = 6.2221 pu.

Bus no.	Bus voltage (pu)		Load (pu)	
1	V_1	1.0939	S_{d1}	0.0000
2	V_2	1.0139	S_{d2}	0.5067
3	V_3	1.0139	S_{d3}	1.9363
4	V_4	0.8893	S_{d4}	0.2716
5	V_5	0.8544	S_{d5}	0.0000
6	V_6	0.9390	S_{d6}	0.9664
7	V_7	0.8544	S_{d7}	0.0000
8	V_8	0.9361	S_{d8}	0.1573
9	V_9	0.8252	S_{d9}	0.6820
10	V_{10}	0.8174	S_{d10}	0.2158
11	V_{11}	0.8441	S_{d11}	0.0793
12	V_{12}	0.8596	S_{d12}	0.1270
13	V_{13}	0.8423	S_{d13}	0.2960
14	V_{14}	0.7997	S_{d14}	0.1653

(3)–(7)} and ranked according lowest values of objective function. Best initial solution (particles) are selected as, Pd_5 = 0.3791 pu, Qd_5 = 0.2015 pu, Pd_3 = 0.1846 pu, Qd_3 = 0.1481 pu, Objective function (J) = 0.6634 pu and λ_{min} = 0.6466. Objective function was evaluated at selected buses using Eq. (1). Table 3 gives the objective function with various combination of DE parameters (α and c_r). Values of DE parameters lie in the range [0, 1]. Maximum numbers of iterations were set equal to 1000. Minimum value of objective function (J) has been obtained for scale factor (α) = 0.70 and crossover probability (c_r) = 0.40. This process is terminated after 649 iterations and no improvement in objective function is noticed. It is observed that all inequality constraints are satisfied and value of proximity indicator is λ_{min} = 0.6207. Table 4 shows comparison of load on load buses and bus voltages; (i) before and after load shedding without optimization, (ii) after optimized load shedding using DE, PSO, and CAPSO [23]. Table 5 gives comparison of optimal load shedding at different buses (bus nos. 5,

Table 8
Load bus ranking according sensitivity of minimum eigenvalue of load flow Jacobian with respect to system load for 14-bus system.

Sr. no.	Load bus	Sensitivity
1	14	0.3155[a]
2	13	0.2609[a]
3	10	0.2511[a]
4	11	0.2460[a]
5	12	0.2339[a]
6	9	0.2163
7	4	0.2108
8	6	0.0469
9	8	0.0449
10	5	0.0000
11	7	0.0000

[a] Load buses selected for load shedding.

Table 9
Effect of DE parameters on optimization of objective function and number of iteration required for convergence for 14-bus test system.

Case	C_r	α	J	No. of Iterations for convergence
1	0.60	0.80	0.3742	617
2	0.65	0.80	0.3812	622
3	**0.55**	**0.80**	**0.3729**	**791**
4	0.50	0.80	0.3756	721
5	0.45	0.80	0.3754	761
6	0.40	0.80	0.3778	782
7	0.65	0.75	0.3739	637
8	0.60	0.75	0.3733	581
9	0.55	0.75	0.3747	677
10	0.50	0.75	0.3771	748
11	0.45	0.75	0.3769	677
12	0.40	0.75	0.3805	564
13	0.65	0.70	0.3833	786
14	0.60	0.70	0.3777	686
15	0.55	0.70	0.3821	739
16	0.50	0.70	0.3834	729
17	0.45	0.70	0.3849	653
18	0.40	0.70	0.3857	649
19	0.65	0.85	0.3925	761
20	0.60	0.85	0.3887	687

Bold face number indicates minimum value of objective function has been achieved in 791 iterations with $C_r = 0.55$ and $\alpha = 0.80$.

3) using DE, PSO and CAPSO techniques. Table 6 gives the comparison of DE, with PSO and CAPSO based on mean value, standard deviation, best value, worst value, frequency of convergence, standard error, length of confidence interval and confidence interval of objective function (Appendix B). Fig. 1 shows a plot between objective function (J) and number of iterations for best values of DE, PSO and CAPSO parameters. Best values of parameters have been selected based on optimum value of objective function. Static voltage stability limit has been obtained using DE, CAPSO and PSO techniques are 2.4789 pu, 2.4622 pu and 2.4581 pu respectively. It is observed that DE algorithm gives much better global optimal results than PSO and its variant coordinated aggregation based particle swarm optimization (CAPSO).

5.2. 14-Bus system

This system consists of three generator buses and eleven load buses. The desired range of load bus voltage is 0.95 pu–1.05 pu. Table 7 shows system load, PV-bus voltages, load bus voltages, value of proximity indicator under simulated stressed condition, and static voltage stability limit. Because of network overloading buses got switched into PQ buses after hitting the maximum limit of their reactive power generation. PV-bus no. 3 has crossed the limit and other PV buses operating very close to their limits. Because of switching from PV bus to PQ bus, the dimension of system Jacobian undergoes a change (increase in dimension). This change in dimension results in drastic change in proximity indicator (sudden decrease); it imposes a challenging task of setting threshold value in algorithm such that desired threshold value of indicator is achieved while considering the fact that these PQ buses will switch back to PV buses after load shedding. In this work a piecewise method is adopted to handle this situation. Set value of indicator is increased in small steps till drastic change (switching back to PV bus) in indicator is observed. From operational experience of system threshold value of indicator is selected as $\lambda_{\min}^{th} = 0.4100$. Table 8 shows evaluated sensitivities at all PQ buses (except at no load PQ buses). Load buses which having highest sensitivities are selected for load shedding. Selected buses are shown as star marked in Table 8. Initially, 3000 populations (0–80% of individual load bus capacity) for each selected load bus have been generated randomly. Continuous power flow was carried out and only 35 sets of particles (Total load is to be shed) of all selected load bus were selected which satisfied all inequality constraints and ranked according lowest values of objective function. Best initial solutions (particles) are selected as $Pd_{14} = 0.0169$ pu, $Qd_{14} = 0.0830$ pu, $Pd_{13} = 0.0936$ pu, $Qd_{13} = 0.0907$ pu, $Pd_{10} = 0.1407$ pu, $Qd_{10} = 0.0875$ pu, $Pd_{11} = 0.0112$ pu, $Qd_{11} = 0.0234$ pu, $Pd_{12} = 0.0008$ pu, $Qd_{12} = 0.0257$ pu, Objective function (J) = 0.4070 pu and $\lambda_{\min} = 0.4317$. Table 9 gives the objective function with various combinations of DE parameters (α and c_r). Maximum numbers of

Table 10
Bus voltages and load on load bus after load shedding with and without optimization techniques for 14-bus test system.

Bus no.	Without optimization				After optimized load shedding					
	Base case		Best initial solution based load shedding		DE		PSO		CAPSO	
	Load (pu)	Voltage (pu)	Load (pu)	Voltage (pu)	Load (pu)	Voltage (pu)	Load (pu)	Voltage (pu)	Load (pu)	Voltage (pu)
1	0.000	1.0939	0.000	1.0939	0.0000	1.0939	0.0000	1.0939	0.0000	1.0939
2	0.5067	1.0139	0.5067	1.0439	0.5067	1.0439	0.5067	1.0439	0.5067	1.0439
3	1.9363	1.0139	1.9363	1.0439	1.9363	1.0339	1.9363	1.0339	1.9363	1.0339
4	0.2716	0.8893	0.2716	1.0251	0.2716	1.0167	0.2716	1.0184	0.2716	1.0182
5	0.0000	0.8544	0.0000	0.9695	0.0000	0.9632	0.0000	0.9633	0.0000	0.9632
6	0.9664	0.939	0.9664	1.0074	0.9664	1.0017	0.9664	1.0023	0.9664	1.0019
7	0.0000	0.8544	0.0000	0.9695	0.0000	0.9632	0.0000	0.9633	0.0000	0.9632
8	0.1573	0.9361	0.1573	1.0013	0.1573	0.9963	0.1573	0.9970	0.1573	0.9964
9	0.6820	0.8252	0.6820	0.9564	0.6820	0.9502	0.6820	0.9500	0.6820	0.9500
10	0.2158	0.8174	0.0501	0.9637	0.0564	0.9572	0.0513	0.9569	0.0340	0.9573
11	0.0793	0.8441	0.0607	0.9895	0.0698	0.9821	0.0646	0.9823	0.0728	0.9824
12	0.1270	0.8596	0.1223	1.0104	0.1228	0.9995	0.1215	1.0033	0.1191	1.0037
13	0.2960	0.8423	0.1803	1.0009	0.2064	0.9905	0.1989	0.9930	0.2553	0.9915
14	0.1653	0.7997	0.1056	0.9628	0.1187	0.9548	0.1165	0.9548	0.1021	0.9539

Table 11
Optimum load shedding at selected load buses using DE, CAPSO and PSO techniques for 14-bus system.

Sr. no.	Optimization techniques	Amount of load shedding at selected load bus										Objective function (pu)
		Bus no. 14		Bus no. 13		Bus no. 10		Bus no. 11		Bus no.12		
		Pd_{14} (pu)	Qd_{14} (pu)	Pd_{13} (pu)	Qd_{13} (pu)	Pd_{10}(pu)	Qd_{10} (pu)	Pd_{11} (pu)	Qd_{11} (pu)	Pd_{12} (pu)	Qd_{12} (pu)	
1	DE	0.0030	0.0907	0.0677	0.0880	0.1297	0.0943	0.0011	0.0288	0.0020	0.0106	0.3729
2	CAPSO	0.0250	0.0724	0.0169	0.1054	0.1556	0.0864	0.0013	0.0242	0.0038	0.0309	0.3782
3	PSO	0.0053	0.0835	0.0749	0.0903	0.1398	0.0868	0.0023	0.0228	0.0016	0.0257	0.3817

Table 12
Comparison of differential evolution method with CAPSO and PSO methods based on statistical inference for 14-bus test system.

Optimization methods	Arithmetic mean value of the objective function ($\bar{J}$)	Standard deviation of objective function (σ)	Best value of objective function (J_{best})	Worst value of objective function (J_{worst})	Frequency of convergence	Confidence level (γ)	Determined value for the engg. application (c)	Standard error of the mean objective function (ε)	Confidence interval of the objective function (μ)	Length of confidence interval of the objective function (L)
DE	0.3796	0.0054	0.3729	0.3925	11	0.95	2.0452	0.0025	$0.3704 \leqslant \mu \leqslant 0.3754$	0.0102
CAPSO	0.3868	0.0058	0.3782	0.3998	09	0.95	2.0452	0.0026	$0.3755 \leqslant \mu \leqslant 0.3808$	0.0109
PSO	0.3895	0.0060	0.3817	0.4038	08	0.95	2.0452	0.0027	$0.3789 \leqslant \mu \leqslant 0.3844$	0.0111

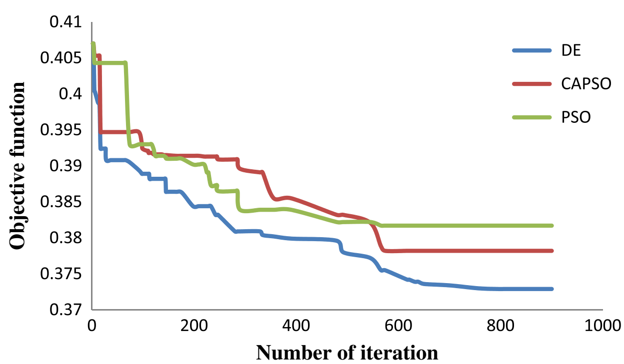

Fig. 2. Plot of convergence of objective function with respect to number of iteration using DE, CAPSO and PSO algorithm for 14-bus system.

iterations were set equal to 1000. Minimum value of objective function (J) has been obtained for scale factor (α) = 0.80 and cross-over probability (c_r) = 0.55. This process is terminated after 791 iterations and no improvement in objective function is noticed. It is observed that all inequality constraints are satisfied and value of proximity indicator is $\lambda_{\min}$ = 0.4182. It is obvious that all PV buses switched, all load bus voltages and line flow are within limit. Table 10 shows comparison of load on load buses and bus voltages; (i) before and after load shedding without optimization, (ii) after optimized load shedding using DE, PSO, and CAPSO. Table 11 gives comparison of optimal load-shed at different buses (bus nos. 10, 11, 12, 13, 14) using DE, PSO and CAPSO techniques. Table 12 gives the comparison of DE, with PSO and CAPSO based on mean value, standard deviation, best value, worst value, frequency of convergence, standard error, length of confidence interval and confidence interval of objective function (Appendix B). Fig. 2 shows a plot between objective function (J) and number of iterations for best values of DE, PSO and CAPSO parameters. Static voltage stability limit has been obtained using differential evolution, CAPSO and PSO techniques are 7.0249 pu, 7.0163 pu and 7.0160 pu respectively.

6. Conclusion

This paper has presented a new algorithm for anticipatory load shedding optimization at selected load buses of the system accounting voltage stability consideration. Load buses have been ranked based on sensitivities of minimum eigenvalue of load flow Jacobian with respect to the load. Load buses have been selected which have large sensitivities for load shedding. The amount of load to be shed at load-bus has been optimized using DE. It is stressed that load shedding is performed at current loading condition. Further, constraints as in Eqs. (3)–(6) are ascertained by performing load flow solution at current operating condition (after load shed) and predicted load condition (accounting load shed). Obtained results using DE have been compared based on mean, standard deviation, best value, worst value, frequency of convergence, standard error of mean, confidence interval and length of confidence interval of objective function, with PSO and its variant. Advantage of DE algorithm is that its mechanization is simple without much mathematical complexity and global optimized solution. It is observed that DE performs much better than PSO and its variant.

Appendix A. Sensitivity derivation of indicator with respect to load shedding at buses

Sensitivity of minimum eigenvalue with respect to real and reactive power changes at a bus is expressed as:

$$\partial\lambda_{\min}/\partial P_i = a_i$$
$$\partial\lambda_{\min}/\partial Q_i = b_i$$

Total change in indicator can be written as follows:

$$\Delta\lambda_{\min} = a_i \cdot \Delta P_i + b_i \cdot \Delta Q_i \quad (A.1)$$

Since when load shed takes place at a bus, then ΔQ_i bears a fixed ratio ΔP_i with (decided by power factor at load bus) as follows:

$$\Delta Q_i = \beta_i \cdot \Delta P_i \quad (A.2)$$

Putting value of ΔQ_i in Eq. 11 change in indicator is obtained as follows:

$$\Delta\lambda_{\min} = (a_i + \beta_i \cdot b_i)\Delta P_i$$
$$\Delta\lambda_{\min} = S_i \cdot \Delta P_i \quad (A.3)$$

where S_i is the $a_i + \beta_i \cdot b_i$, β_i is $\tan\phi_i$, ϕ_i is power factor angle at ith load bus, and $\lambda_{\min}$ is the minimum eigenvalue of load flow Jacobian.

Expression for a_r and b_r can be written as follows [24]:

$$a_r = \partial\lambda_{\min}/\partial P_r = \sum_{ij}(\partial\lambda_{\min}/\partial H_{ij})(\partial H_{ij}/\partial P_r) + \sum_{ij}(\partial\lambda_{\min}/\partial N_{ij})(\partial N_{ij}/\partial P_r) + \sum_{ij}(\partial\lambda_{\min}/\partial M_{ij})(\partial M_{ij}/\partial P_r) + \sum_{ij}(\partial\lambda_{\min}/\partial L_{ij})(\partial L_{ij}/\partial P_r) \quad (A.4)$$

$$b_r = \partial\lambda_{\min}/\partial Q_r = \sum_{ij}(\partial\lambda_{\min}/\partial H_{ij})(\partial H_{ij}/\partial Q_r) + \sum_{ij}(\partial\lambda_{\min}/\partial N_{ij})(\partial N_{ij}/\partial Q_r) + \sum_{ij}(\partial\lambda_{\min}/\partial M_{ij})(\partial M_{ij}/\partial Q_r) + \sum_{ij}(\partial\lambda_{\min}/\partial L_{ij})(\partial L_{ij}/\partial Q_r) \quad (A.5)$$

where H_{ij}, N_{ij}, M_{ij}, L_{ij} are the elements of sub-Jacobian of load flow defined as follows:

$$J' = \begin{bmatrix} H & N \\ M & L \end{bmatrix} \quad (A.6)$$

Expression for elements of sub-Jacobian can be written as follows:

$$H_{ij} = V_i \cdot V_j \cdot Y_{ij} Sin(\delta_i - \delta_j - \theta_{ij}) \quad (A.7)$$

$$H_{ii} = -Q_i - V_i^2 \cdot B_{ii} \quad (A.8)$$

$$N_{ij} = V_i \cdot Y_{ij} Cos(\delta_i - \delta_j - \theta_{ij}) \quad (A.9)$$

$$N_{ii} = G_{ii} \cdot V_i + P_i/V_i \quad (A.10)$$

$$M_{ij} = -V_i \cdot V_j \cdot Y_{ij} Cos(\delta_i - \delta_j - \theta_{ij}) \quad (A.11)$$

$$M_{ii} = P_i - G_{ii}V_i^2 \quad (A.12)$$

$$L_{ij} = V_i \cdot Y_{ij} Sin(\delta_i - \delta_j - \theta_{ij}) \quad (A.13)$$

$$L_{ii} = Q_i/V_i - B_{ii}V_i \quad (A.14)$$

where Y_{ij} and θ_{ij} are magnitude and angle of ijth element of bus admittance matrix.

Following relations are observed from minimum eigenvalue sensitivity theory of matrices [25].

$$\partial\lambda_{\min}/\partial H_{ij} = \eta_i \cdot \xi_j \quad (A.15)$$

$$\partial\lambda_{\min}/\partial N_{ij} = \eta_i \cdot \xi_{(j+NB-1)} \quad (A.16)$$

$$\partial\lambda_{\min}/\partial M_{ij} = \eta_{(i+NB-1)} \cdot \xi_j \quad (A.17)$$

$$\partial\lambda_{\min}/\partial L_{ij} = \eta_{(i+NB-1)} \cdot \xi_{(j+NB-1)} \quad (A.18)$$

where η and $.\xi$ are left and right eigen vectors corresponding to minimum eigenvalue of load flow Jacobian. $\eta_{(\cdot)}$ and $.\xi_{(\cdot)}$ are corresponding elements. Partial derivatives of Schur's inequality proximity indicator w.r.t. sub-components of load flow Jacobian (H_{ij}, N_{ij}, M_{ij}, L_{ij}) have been evaluated. Expression for other partial derivatives in Eqs. (A.4) and (A.5) are obtained as follows:

$$\partial H_{ij}/\partial P_r = V_i \cdot V_j \cdot Y_{ij} Cos(\delta_{ij} - \theta_{ij})[S_{1ir} - S_{1jr}] + Y_{ij} Sin(\delta_{ij} - \theta_{ij})[V_j \cdot S_{3ir} + V_i \cdot S_{3jr}]$$
$$\partial H_{ij}/\partial Q_r = V_i \cdot V_j \cdot Y_{ij} Cos(\delta_{ij} - \theta_{ij})[S_{2ir} - S_{2jr}] + Y_{ij} Sin(\delta_{ij} - \theta_{ij})[V_j \cdot S_{4ir} + V_i \cdot S_{4jr}]$$
$$\partial H_{ii}/\partial P_r = -2B_{ii} \cdot V_i \cdot S_{3ir}$$
$$\partial H_{ii}/\partial Q_r = -2B_{ii} \cdot V_i \cdot S_{4ir}$$
$$\partial N_{ij}/\partial P_r = Y_{ii} Cos(\delta_i - \delta_j - \theta_{ij}) \cdot S_{3ir} - V_i \cdot Y_{ij} Sin(\delta_i - \delta_j - \theta_{ij})[S_{1ir} - S_{1jr}]$$
$$\partial N_{ij}/\partial Q_r = Y_{ii} \cdot Cos(\delta_i - \delta_j - \theta_{ij}) \cdot S_{4ir} - V_i \cdot Y_{ij} Sin(\delta_i - \delta_j - \theta_{ij})[S_{2ir} - S_{2jr}]$$
$$\partial N_{ii}/\partial P_r = G_{ii} \cdot S_{3ir} - \left(P_r/V_i^2\right) \cdot S_{3ir}$$
$$\partial N_{ii}/\partial Q_r = G_{ii} \cdot S_{4ir} - \left(P_r/V_i^2\right) \cdot S_{4ir}$$
$$\partial M_{ij}/\partial P_r = V_i \cdot V_j \cdot Y_{ij} Sin(\delta_i - \delta_j - \theta_{ij})[S_{1ir} - S_{1jr}] - Y_{ij} Cos(\delta_i - \delta_j - \theta_{ij})[V_i \cdot S_{3jr} + V_j \cdot S_{3ir}]$$
$$\partial M_{ij}/\partial Q_r = V_i \cdot V_j \cdot Y_{ij} Sin(\delta_i - \delta_j - \theta_{ij})[S_{2ir} - S_{2jr}] - Y_{ij} Cos(\delta_i - \delta_j - \theta_{ij})[V_i \cdot S_{4jr} + V_j \cdot S_{4ir}]$$
$$\partial M_{ii}/\partial P_r = -2G_{ii} \cdot S_{3ir}$$
$$\partial M_{ii}/\partial Q_r = -2G_{ii} \cdot V_i \cdot S_{4ir}$$
$$\partial L_{ij}/\partial P_r = V_i \cdot Y_{ij} Cos(\delta_i - \delta_j - \theta_{ij})[S_{1ir} - S_{1jr}] + Y_{ij} Sin(\delta_i - \delta_j - \theta_{ij}) \cdot S_{3ir}$$
$$\partial L_{ij}/\partial Q_r = V_i \cdot Y_{ij} Cos(\delta_i - \delta_j - \theta_{ij})[S_{2ir} - S_{2jr}] + Y_{ij} Sin(\delta_i - \delta_j - \theta_{ij}) \cdot S_{4ir}$$
$$\partial L_{ii}/\partial P_r = -\left[\left\{\left(Q_i/V_i^2\right) + B_{ii}\right\} \cdot S_{3ir}\right]$$
$$\partial L_{ii}/\partial Q_r = -\left[\left\{\left(Q_i/V_i^2\right) + B_{ii}\right\} \cdot S_{4ir}\right]$$

In the above partial derivative evaluation expression S_{1ir}, S_{1jr}, S_{2ir}, S_{2jr}, S_{3ir}, S_{3jr}, S_{4ir} and S_{4jr} are elements of sub- sensitivity matrixes [S_1–S_4] obtained by the inversion of [J'] as follows;

$$[J']^{-1} = \begin{bmatrix} S_1 & S_2 \\ S_3 & S_4 \end{bmatrix}$$

Inversion of Jacobian is obtained using optimally ordered factorization (OOF) technique [26,27].

Appendix B. Confidence interval and length of confidence interval [28]

Obtain confidence interval and length of confidence interval using following steps:

Step-1: Arithmetic means value of the objective function:

$$\bar{J} = \left[1/n\sum_{j=1}^{n}(J_j)\right] \tag{B.1}$$

Step-2: Standard deviation of objective function:

$$\sigma = [\{1/(n-1)\}\sum_{j=1}^{n}(J_j - \bar{J})^2]^{1/2} \tag{B.2}$$

Step-3: Confidence level $(\gamma) = 0.95$

$c = 2.0452$

Step-4: Standard error of the mean objective function

$$(\varepsilon) = c\sigma/\sqrt{n} \tag{B.3}$$

Step-5: Confidence interval of the objective function

$$[(\bar{J} - \varepsilon) \leqslant \mu \leqslant (\bar{J} + \varepsilon)] \tag{B.4}$$

Step-6: Length of confidence interval

$$(L) = [(\bar{J} + \varepsilon) - (\bar{J} - \varepsilon)]c = 2\varepsilon c \tag{B.5}$$

References

[1] Shokooh F, Dai JJ, Shokooh S, Taster J, Castro H, Khantelwal T, et al. An intelligent load shedding (ILS) system application in a large industrial facility. In: Proc. 14th IAS Annual Meeting. vol. 1; 2005. p. 417–25.
[2] Wiszniewski A. New criteria of voltage stability margin for the purpose of load shedding. IEEE Trans Power Syst 2007;22(3):1367–71.
[3] Taylor CW. Concept of under voltage load shedding for voltage stability. IEEE Trans Power Delivery 1992;7(2):480–7.
[4] Chuvychin VN, Gurov NS, Venkta SS, Brown RE. An adaptive approach to load shedding and spinning reserve control during under frequency conditions. IEEE Trans Power Syst 1996;11(6):1805–10.
[5] Shah S, Shahidehpour SM. A heuristic approach to load shedding scheme. IEEE Trans Power Syst 1989;4(4):1421–9.
[6] Berg GJ, Sharaf TA. System load ability and load shedding. Electr Power Syst Res 1994;28:217–25.
[7] Tuan TQ, Fandino J, Hadjsaid N, Sabonnadiere JC, Vu H. Emergency load shedding to avoid risk of voltage instability using indicators. IEEE Trans Power Syst 1994;19(1):341–51.
[8] El-Sadek MZ, Mahomod GA, Dessouky MM, Rashed WI. Optimum load shedding for avoiding study state voltage instability. Electr Power Syst Res 1999;15(2):119–23.
[9] Bijwe PR, Tare RS, Kelapure SM. Anticipatory load shedding scheme for loadability enhancement. IEE Proc GTD 1999;146(3):483–90.
[10] Luan WP, Irving MR, Daniel JS. Genetic algorithm for supply restoration and optimal load shedding in power system distribution networks. IEE Proc GTD 2002;149(2):145–51.
[11] Jung J, Liu C-C, Tanimoto Steven L, Vittal V. Adoption in load shedding under vulnerable operating condition. IEEE Trans Power Syst 2002;17(4):1199–205.
[12] Echavarren FM, Lobato E, Rouco L. A corrective load shedding scheme to mitigate voltage collapse. Int J Electr Power Energy Syst 2006;28:58–64.
[13] Chattopadhyay D, Chakraborti BB. A preventive/corrective model for voltage stability incorporating dynamic load shedding. Int J Electr Power Energy Syst 2003;25:363–76.
[14] Amraee T, Ranjbar AM, Mozafari B, Sadati N. An enhance under voltage load shedding scheme to provide voltage stability. Electr Power Syst Res 2007;77:1038–46.
[15] Girgis A, Mathure S. Application of active power sensitivity to frequency and voltage variations on load shedding. Electr Power Syst Res 2010;80(3):306–10.
[16] Fu Xu, Wang Xifan. Determination of load shedding to provide voltage stability. Int J Electr Power Energy Syst 2011;33(3):515–21.
[17] Amraee T, Ranjbar AM, Feuillet R. Adaptive under-voltage load shedding scheme using model predictive control. Electr Power Syst Res 2011;81(7):1507–13.
[18] Storn R, Price K. Differential evolution – a simple and efficient adaptive scheme for global optimization over continuous spaces. Technical report TR-95012, ICSI.
[19] Price K, Storn R, Lampinen J. Differential evolution: a practical approach to global optimization. Springer; 2005.
[20] Tvrdik J. Adoption in differential evolution: a numerical comparison. Appl Soft Comput J 2009;9(3):1149–55.
[21] Lampinen J. A constraint handling approach for differential evolution algorithm. In: Proc. of 2002 congress on evolutionary computation (CEC-2002). vol. 2. p. 1468–73.
[22] Bijwe PR, Kothari DP, Arya LD. Alleviation of line over loads and voltage variations by corrective rescheduling. IEEE Proc Part-C 1993;140(4):249–55.
[23] Arya LD, Choube SC, Shrivastava M, Kothari DP. Loadability margin enhancement using co-ordinated aggregation based particle swarm optimization (CAPSO). Int J Electr Power Energy Syst 2010;32(9):975–84.
[24] Lima PEF. A sensitivity analysis of eigen structure. IEEE Trans Power Syst 1997;12(3):1393–9.
[25] Chandekar SM, Tarnekar SG. Revised load shedding schedule for power system incorporating the effect of transmission line performance. Electric Power Energy Syst 2002;24:379–86.
[26] Tinney WF, Walker JW. Direct solution of sparse network equations by optimally ordered factorization. IEEE Proc 1967;55:1801–5.
[27] Wallach Y. Calculations and program for power system networks. Englewood Cliffs, NJ: Prentice-Hal, Inc.; 1986. Book.
[28] Kreyszig EW. Advance engineering mathematics. John Wiley & Sons, Inc.; 2001. Book.